

Modulation of the venation pattern of cotyledons of transgenic tobacco for the tumorigenic *6b* gene of *Agrobacterium tumefaciens* AKE10

Yasutaka Kakiuchi · Sachiko Takahashi · Hiroetsu Wabiko

Received: 8 August 2006 / Accepted: 1 October 2006 / Published online: 30 November 2006
© The Botanical Society of Japan and Springer 2006

Abstract Neoplastic plant-tissue formation, termed crown gall disease, is induced on infection with *Agrobacterium tumefaciens*. The tumorous tissues develop an extensive vascular system, with a venation pattern distinct from that of native host plants. We report here that the plant-tumorigenic *6b* gene of the *A. tumefaciens* strain AKE10 is capable of inducing extensive vein formation in transgenic tobacco seedlings with distinct pattern formation. Unlike the wild-type cotyledons, transgenic cotyledons had wavy and striate veins depending on the extent of severity of leaf morphology. Graph analysis of the transgenic cotyledonous vein patterns revealed an increase in the number of branch points of veins, end-points of veins, and areas surrounded by the veins. Histological analysis showed abnormal tissue growth on the abaxial side of the cotyledon blades and continual formation of adventitious veins. These adventitiously formed veins included inverted dorso-ventrality and formation of a radial axis.

Keywords Cotyledon · Dorso–ventral axis · *Nicotiana tabacum* · *6b* gene · Venation pattern

Y. Kakiuchi · S. Takahashi · H. Wabiko (✉)
Faculty of Bioresource Sciences,
Akita Prefectural University, Nishi 241-438,
Nakano-Aza Kaidobata, Shimoshinjo,
Akita 010-0195, Japan
e-mail: wabi@akita-pu.ac.jp

Y. Kakiuchi
Cell Biology and Biochemistry, Faculty of Science,
Ochanomizu University, 2-1-1 Otsuka, Bunkyo-ku,
Tokyo 112-8610, Japan

Introduction

The vascular systems of cotyledons and the leaves of plants are genetically well defined and are characteristic of individual plant species. Among a number of plant-growth regulators, auxin plays a crucial role in both induction and pattern formation of vascular systems (Aloni 1995; Fukuda 1992; Sachs 1989; Nelson and Dengler 1997). Polar auxin transport, which is regulated by influx and efflux carriers, is also important in determining vascular pattern formation. Application of specific inhibitors against auxin transport induces extensive generation of vascular bundles and modulation of vein pattern (Sieburth 1999; Mattsson et al. 1999, 2003). Auxin transport mutant *lop1* of *Arabidopsis* also has altered vascular patterning including midvein bifurcation and rotation (Carland and McHale 1996). Two main hypotheses have been proposed to explain vascular pattern formation:

- the signal flow canalization hypothesis, in which vascular development is thought to be induced along the path of auxin flow (Sachs 1981, 1989; Feugier et al. 2005), and
- the reaction–diffusion (RD) hypothesis, in which hypothetical diffusible products, comprising positive and negative regulators, determine the venation pattern (Meinhardt 1982; Koizumi et al. 2000).

Crown gall formation is induced in plants on infection with the soil bacterium, *Agrobacterium tumefaciens*. During infection with *A. tumefaciens*, the T-DNA (transferred DNA) of the tumor-inducing plasmid (Ti-plasmid) harbored by the bacterium is transferred and integrated into the host plant chromosome (Van Larebeke et al. 1974; Chilton et al. 1977). The T-DNA

contains the biosynthesis genes for auxin (*iaaM*, Van Onckelen et al. 1986; Thomashow et al. 1986; *iaaH*, Thomashow et al. 1984; Schröder et al. 1984) and cytokinin (*ipt* gene, Akiyoshi et al. 1984), and several accessory genes, for example gene 5 and gene 6*b*, which are known to modulate the action of auxin and/or cytokinin (Körber et al. 1991; Spanier et al. 1989; Tinland et al. 1989; Gális et al. 1999). The expression of these hormonal and accessory genes is responsible for tumorigenic cell proliferation and ectopic vascular formation of crown galls. The resulting tumorous outgrowths seem to comprise a mass of undifferentiated or teratoma-forming callus tissues. Considering such massive cell proliferation, which escapes growth regulation by the host plants, it is striking that a unique and partially organized venation pattern develops inside the crown gall tissues; one is composed of a radial arrangement along the apical–basal axis with each vein aligned in parallel toward the tip of the gall (Aloni et al. 1995).

The 6*b* gene has been shown to induce tumors in a limited number of host plant species (Hooykaas et al. 1988). In transgenic tobacco, expression of the 6*b* gene (AK-6*b*), obtained from strain AKE10, induced several distinct morphological alterations and elevated accumulation of phenylpropanoids, including some flavonoids (Wabiko and Minemura 1996; Gális et al. 2002, 2004). More recently we have found that polar auxin transport activity is reduced in these transgenic tobacco seedlings (Kakiuchi et al. 2006). Because a group of naturally occurring flavonoids has been reported to perturb auxin transport (Jacobs and Rubery 1988), it is most likely that greater accumulation of flavonoids in the AK-6*b*-tobacco affected polar auxin transport. Here, we investigated venation pattern formation of morphologically altered AK-6*b*-tobacco seedlings. A reduced level of auxin transport may have modified distribution of auxin, which could account for the extensive vascular systems.

Materials and methods

Plant materials and growth conditions

The AK-6*b* gene, placed under the control of the dexamethasone (Dex)-inducible promoter (Aoyama and Chua 1997), was introduced into tobacco, *Nicotiana tabacum* cv. Samsun to generate the line 6*b*-S9 (Kakiuchi et al. 2006). This line seemed to contain two copies of the transgene as determined by phenotypic segregation analysis (Kakiuchi et al. 2006). Seeds obtained from the primary 6*b*-S9 line were sown and left

to grow on MS (Murashige and Skoog) medium containing 10 $\mu\text{mol L}^{-1}$ Dex and 50 $\mu\text{g mL}^{-1}$ hygromycin without auxin or cytokinin at 25°C under a 16 h-light and 8 h-dark cycle.

Venation pattern analysis

Veins of cotyledons were visualized according to Kozumi et al. (2000) by fixation of samples overnight in a mixture of ethanol–acetic acid, 3:1 (v/v), then clarification in chloral hydrate–glycerol–water, 8 g:1 mL:2 mL. Microscopic photographs were taken with a digital camera (Nikon, Japan) and the vein patterns were extracted from digital images by manually tracing the vein profiles using Photoshop software (Adobe, Tokyo, Japan). The length of the veins and the leaf area were determined from the extracted vein patterns after skeletonization by an image-processing program (Scion Image, Scion Corporation, MD, USA, available on the Internet at <http://www.scioncorp.com/>).

Histological analysis

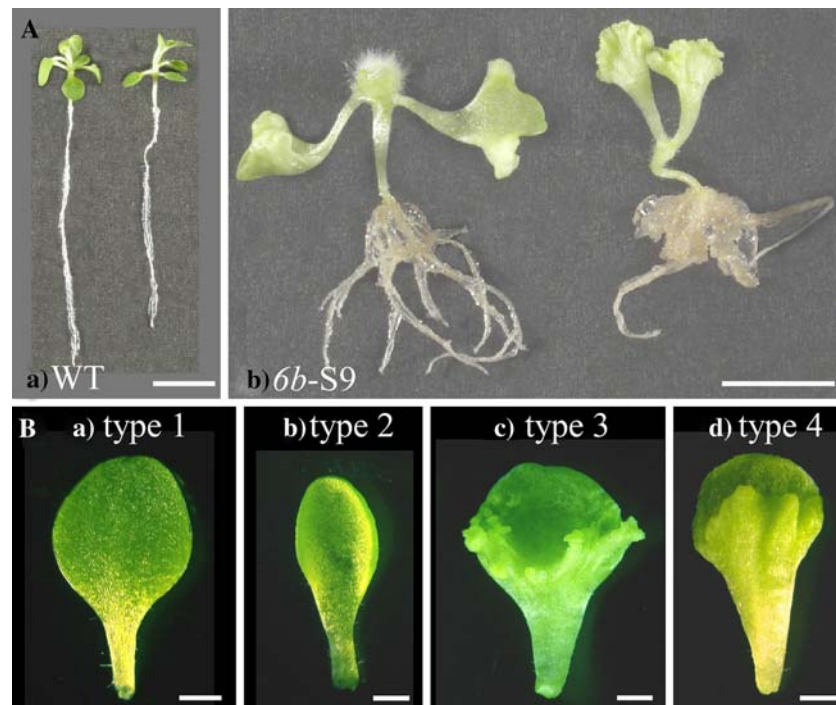
Plant materials were fixed overnight in FAA solution composed of formalin–acetic acid–ethanol–water, 5:5:45:45 (v/v), at room temperature. Fixed samples were dehydrated by immersion in a series of ethanol–tertiary (*t*)-butanol solutions, with increasing *t*-butyl alcohol fractions, and, finally, in pure *t*-butanol. Tissues were then vacuum-infiltrated and embedded in paraffin. Subsequently, 8- μm tissue sections were prepared and stained with 5% (w/v) toluidine blue. To visualize the lignin content the sections were stained with a mixture of 1.3% (w/v) phloroglucinol in ethanol–hydrochloric acid, 67:6 (v/v).

Results

Excessive vascular formation in transgenic cotyledons

The seedlings of the T1 generation of the primary line 6*b*-S9 were classified into four distinct phenotypic groups on the basis of cotyledon morphology, as reported by Kakiuchi et al. (2006) (Fig. 1). In brief, type 1 was of normal morphology and indistinguishable from wild-type seedlings (Fig. 1Ba); type 2 showed hyponasty (Fig. 1Bb); type 3 displayed hyponasty and adventitious outgrowths at the lateral margins on the abaxial side of the blade (Fig. 1Bc), and, in contrast, type 4 showed increased epinasty and adventitious outgrowths in the central portion of the abaxial side of

Fig. 1 Morphologies of whole seedlings and cotyledons of transgenic tobacco expressing the AK-6*b* gene. Seedlings were grown on MS medium containing $10 \mu\text{mol L}^{-1}$ Dex with (transgenics) or without (wild-type) $50 \mu\text{g mL}^{-1}$ hygromycin. **A** 24-day-old seedlings of wild-type control (panel a) and the AK-6*b*-transgenic tobacco line 6*b*-S9 (panel b). Scale bars: 1 cm. **B** Cotyledons of 18-day-old 6*b*-S9 seedlings of type 1 (panel a), type 2 (panel b), type 3 (panel c), and type 4 (panel d). Scale bars: 1 mm



the blade (Fig. 1Bd). The extent of the observed abnormalities correlated well with AK-6*b* transcript levels (Kakiuchi et al. 2006).

Because plant vascular formation is a sensitive guide for evaluating morphological abnormalities of cotyledons, we investigated the patterns of venation in transgenic cotyledons on AK-6*b* gene expression. Visual inspection of the distribution of entire vascular bundles in the cotyledons revealed that the venation patterns of type 1 and wild-type were topologically equivalent and remained unchanged from 10 days until 22 days after sowing on the growth medium (Fig. 2A, data not shown). In contrast, cotyledons of types 2–4 seemed to have progressively more complex patterns that became even more complex with increasing incubation time (Figs. 2B–G). Closer examination revealed that virtually all the veins in the type 2 cotyledons became tortuous (Figs. 2B, C). Occasionally, the thick mid-vein could not be distinguished from the remaining veins immediately after branching away from the petiole-cotyledon junction (Fig. 2C). Excessive veins were more prominent in the type 3 and type 4 cotyledons than in type 2, resembling the striated (striped) pattern extending to the outgrowth margins and comprising a complex three-dimensional network (Figs. 2D–G).

Although vein pattern formation was dramatically altered in the transgenic seedlings, the extent of lignin deposition in the tracheary elements of the type 3 vascular vessels seemed similar to that of wild-type

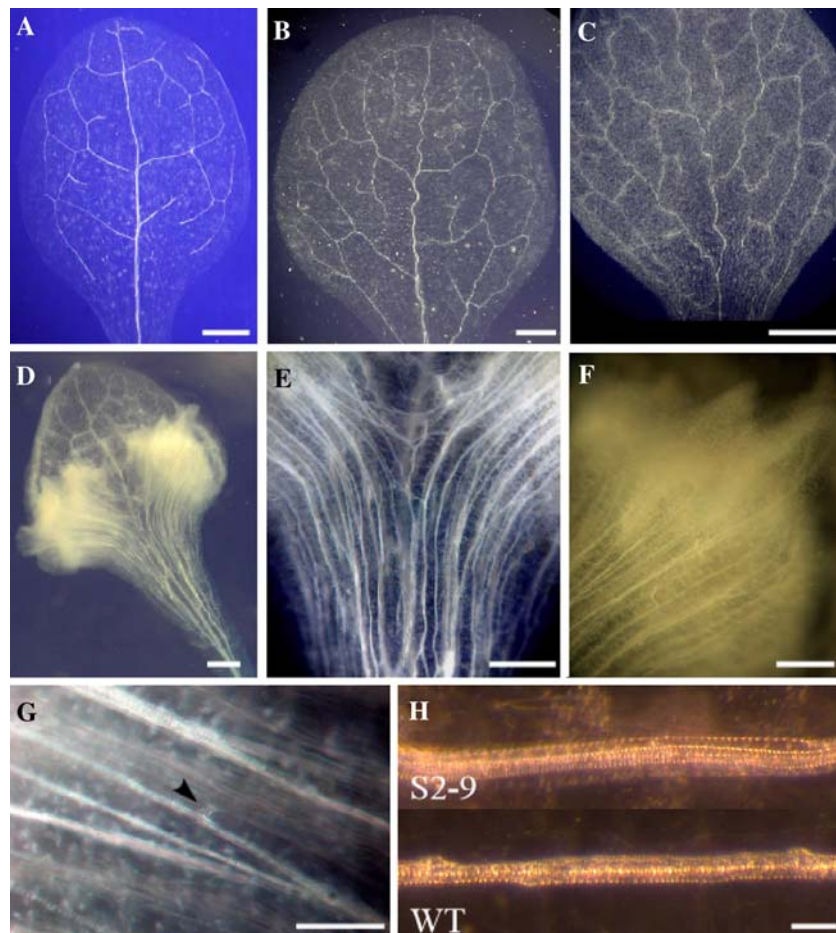
controls (Fig. 2H), suggesting that the molecular basis for the chemical and physical structure of the tracheary elements was normal.

Quantitative analysis of venation complexity of transgenic cotyledons

To analyze the venation patterns quantitatively we determined the total lamina area (area) and total length of veins (total venation) of the cotyledons throughout development (Figs. 3A, Ba, Bb), and thereby calculated the venation density as the total vein length divided by the lamina area (Fig. 3Bc). We also determined several graph parameters: the number of branching points (# Branch), the number of end-points that were not contiguous with adjacent veins (# Free-end), and the number of regions enclosed within surrounding veins (# Areole), all of which were represented as individual values per cotyledon (Figs. 3Bd–Bf).

The development of type 1 and wild-type cotyledons reached maturation after approximately 10 days and so the area of both cotyledons remained constant during the subsequent 10 to 22-day period (Fig. 3Ba). The area and total venation of the type 1 cotyledons were always slightly larger and longer, respectively, than those of the wild-type cotyledons. The resulting venation density remained constant and at equivalent levels in the type 1 and wild-type cotyledons, however

Fig. 2 Vascular bundles in cotyledons. Wild-type (Samsun) and transgenic (*6b-S9* line) tobacco seedlings were treated with Dex, and the cotyledons then excised, fixed and cleared with chloral hydrate. The vascular bundles were visualized by dark-field microscopy. **A** Wild-type 22-day-old seedlings. **B, C** Type 2 seedlings from the *6b-S9* line treated with Dex for 16 days (**B**) and 22 day (**C**). **D–G** Type 3 seedlings from 22-day-old *6b-S9* line. Vascular bundles (**D**) were magnified at the junction of the petiole and leaf blade (**E, G**), and at the periphery of lateral outgrowth (**F**). The right-side vein in panel **F** is obscure because illumination was overshadowed by other veins. An *arrowhead* in panel **G** (a higher magnification of panel **F**) denotes a commissural vein interconnecting the two parallel veins on both sides. **H** Lignin was stained with phloroglucinol. *Scale bars*: 1 mm in **A–C** and **F**; 2 mm in **D** and **E**; 0.5 mm in **G**; 0.1 mm in **H**



(Figs. 3A, Ba–Bc). Graph parameters were, furthermore, also indistinguishable between the type 1 and wild-type cotyledons (Fig. 3Bd–Bf). Thus, type 1 cotyledons were comparable with wild-type cotyledons in respect of both venation density and venation pattern.

A more extensive increase in leaf area was observed for the type 2 cotyledons (Fig. 3Ba) than for the type 1 cotyledons, and yet their venation density remained constant and at levels equivalent to the wild-type and type 1 cotyledons, because of the concomitant increases in total venation (Figs. 3Ba–Bc). Graph analysis revealed, however, that the type 2 vein pattern was quite distinct from that of the type 1 and wild-type cotyledons. It should be noted that the graph parameters of the venation patterns for type 2–4 cotyledons were already different from those of wild-type and type 1 cotyledons as early as 6 days, corresponding to 2–3 days after germination, when large parts of the cotyledons were still wrapped within the seed coats and only simple venation patterns could be observed (Figs. 3Bd–Bf, also see below). Graph parameters for cotyledons of all these three plant types increased with time and reached maximum levels after 8 to 10 days

(Figs. 3Bd–Bf), and the rates of increase and the maximum values of # Branch, # Free-end, and # Areole were nearly twice those for type 1 and wild-type cotyledons (Figs. 3Bd–Bf). The venation density of type 2 cotyledons was therefore normal, but the venation pattern was distinct from that of wild-type seedlings.

In the type 3 and 4 cotyledons before the development of the adventitious outgrowths (at 10 days) the venation patterns were already complex and most probably different from that of type 2 cotyledons (Figs. 3Bd–Bf). As cotyledon development proceeded, the venation patterns became denser and comprised intricate three-dimensional networks in association with increasing growth rate (Figs. 3A, at 16 and 22 days), together with higher venation densities, than those of the corresponding type 1, type 2, and wild-type cotyledons (Fig. 3Bc). On development of the outgrowths of the type 3 and 4 cotyledons, the increased venation complexity was much more prominent in the outgrowths, thus rendering graph analysis impossible for the fully developed outgrowths (22 days, Figs. 3A, Bd–Bf). Hence, type 3 and type 4 cotyledons had prominently abnormal venation density and venation

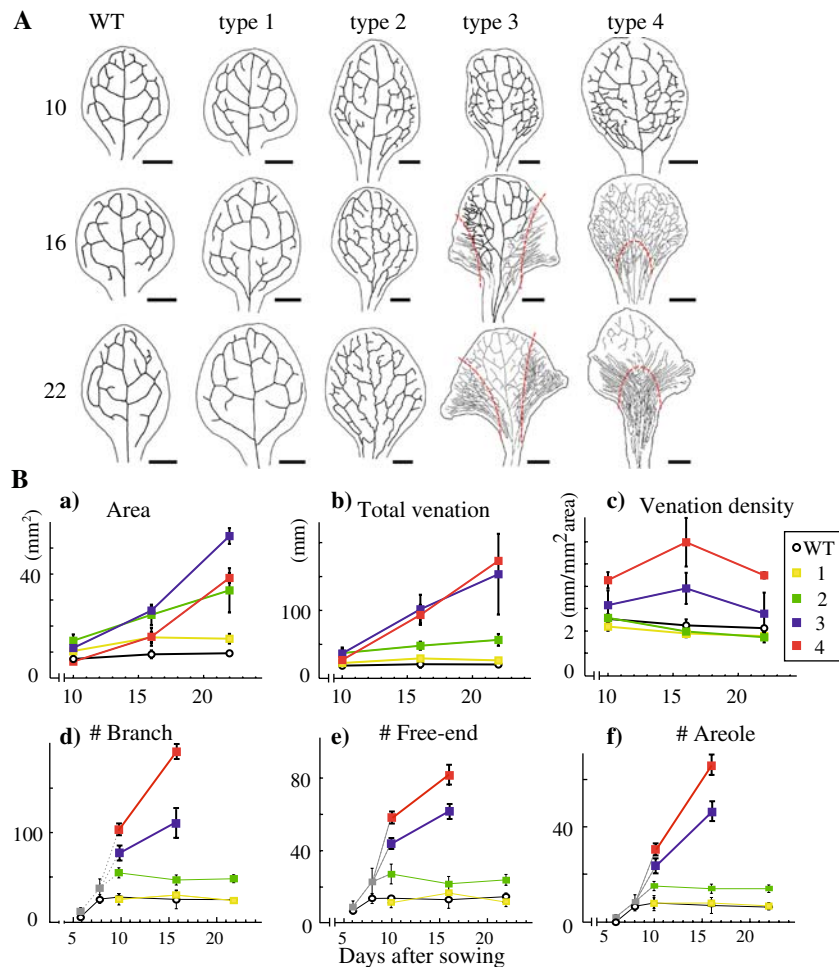


Fig. 3 Schematic and graph analysis of venation in cotyledons. **A** Schematic illustration of venation patterns in 10, 16, and 22-day-old cotyledons of wild-type control and transgenic (6b-S9) seedlings. Dotted red lines show the boundaries between cotyledons and outgrowths. For the 16 and 22-day-old type 3 and 4 cotyledons the venations were so complex that most of the fine venations are not drawn. Different scales are used for convenient comparison. **B** Time course of graph indexes. The entire cotyledonous leaf area (a), total vein length (b), and venation density (c; vein length divided by area), were determined for wild-type (black), type 1 (yellow), type 2 (green), type 3 (blue), and type 4 (red) seedlings. Graph parameters for

the total number of branching points (d), total number of free-ends of veins (e), and the number of areoles (f), all of which are represented as numbers per cotyledon in the ordinates, were determined by manual tracing of the images shown in **A**. Because of the highly complex venation patterns of the type 3 and 4 cotyledons, the total vein length (b) and venation density (c) are substantially underestimated and the graph indexes d, e and f, could not be determined for these types. Graph values of the type 2–4 cotyledons before 10 days are shown by dotted gray lines. During this period the typical group types were indistinguishable because of the lack of outgrowths from the type 3 and 4 cotyledons at this stage of development

pattern at both the early and late stages of cotyledon and outgrowth development.

Modulated dorsoventral pattern in the outgrowths

We performed histological analysis of the fully developed, aberrant morphologies of the transgenic cotyledons. Transverse sections were made of the middle portions of wild-type, type 2 and 3 cotyledon leaf blades and of the basal part (proximal to the petiole) of the type 4 transgenic cotyledons (Fig. 4B; diagrams are depicted in Fig. 4A). In wild-type cotyledons, spongy

tissue and palisade tissue were both distinguishable, whereas in types 2–4 these cells were morphologically altered and both indistinguishable in mesophyll cell layers. The distance between the individual vascular bundles and the adaxial epidermis was relatively constant among wild-type and transgenic cotyledons whereas the distance between the vascular bundles and the abaxial epidermis was increased in type 3 and 4 cotyledons in comparison with the corresponding distance in wild-type, type 1, type 2 cotyledons. In particular, preferential cell proliferation of both epidermal and mesophyll cells of the abaxial side was evident

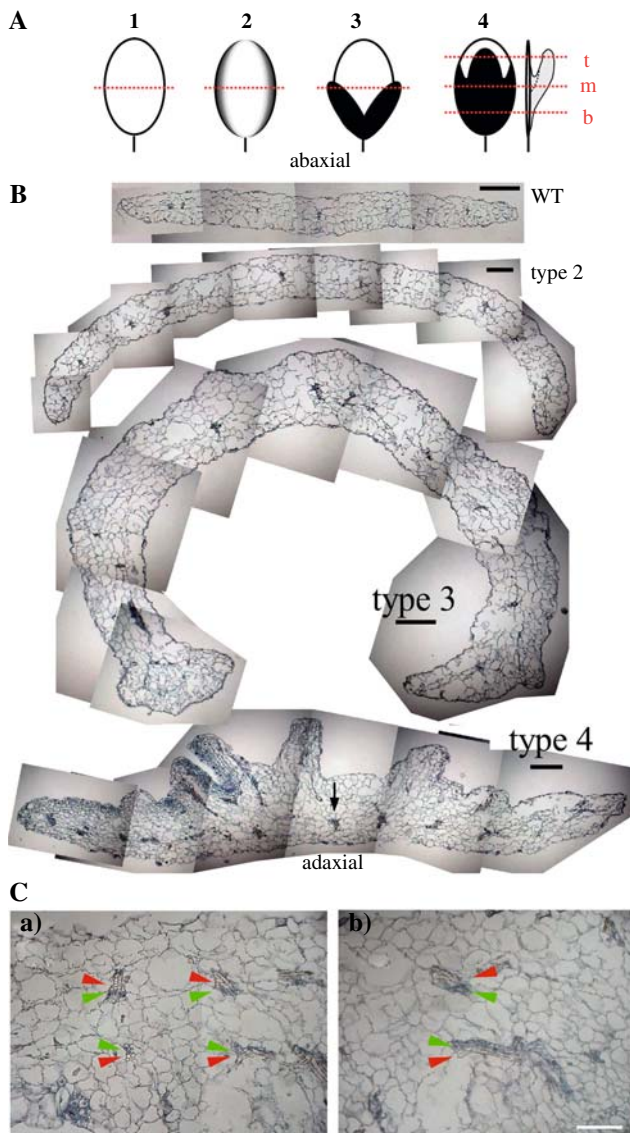


Fig. 4 Histological analysis of wild-type (Samsun) and transgenic (*6b-S9*) cotyledons. Seedlings were grown on MS medium containing Dex with (transgenics) or without (wild-type) hygromycin for 24 days. **A** Schematic diagrams showing front view (types 1–4) and side view (type 4) of the cotyledons with *horizontal lines* illustrating the position where sections were made for histological analysis. For types 1–3, single sections were made at the middle part, and for type 4, three sections were made at the basal (*b*), middle (*m*) and tip (*t*) parts of the cotyledons; these are illustrated in **B** and **C** and in Figs. 5A, C. Epinastic curvature in type 2 cotyledon is drawn as *graded margin*, and outgrowths in types 3 and 4 are drawn as *solid area*. **B** Transverse sections of wild-type and transgenic cotyledons were made at the position shown above and stained with toluidine blue. For type 4, a section made from the basal region (*line b* in **A**) comprising the cotyledon and outgrowth is shown. Pictures are shown with the abaxial surface upper side in the panels. An *arrow* indicates a cotyledonous vein. *Scale bars*: 0.5 mm. **C** Adventitiously formed veins with inverted dorsoventrality at the basal region of type 4 cotyledons. *Red* and *green arrowheads* denote xylem and phloem, respectively. The abaxial side corresponds to the upper side of the panel. *Scale bar*: 0.2 mm

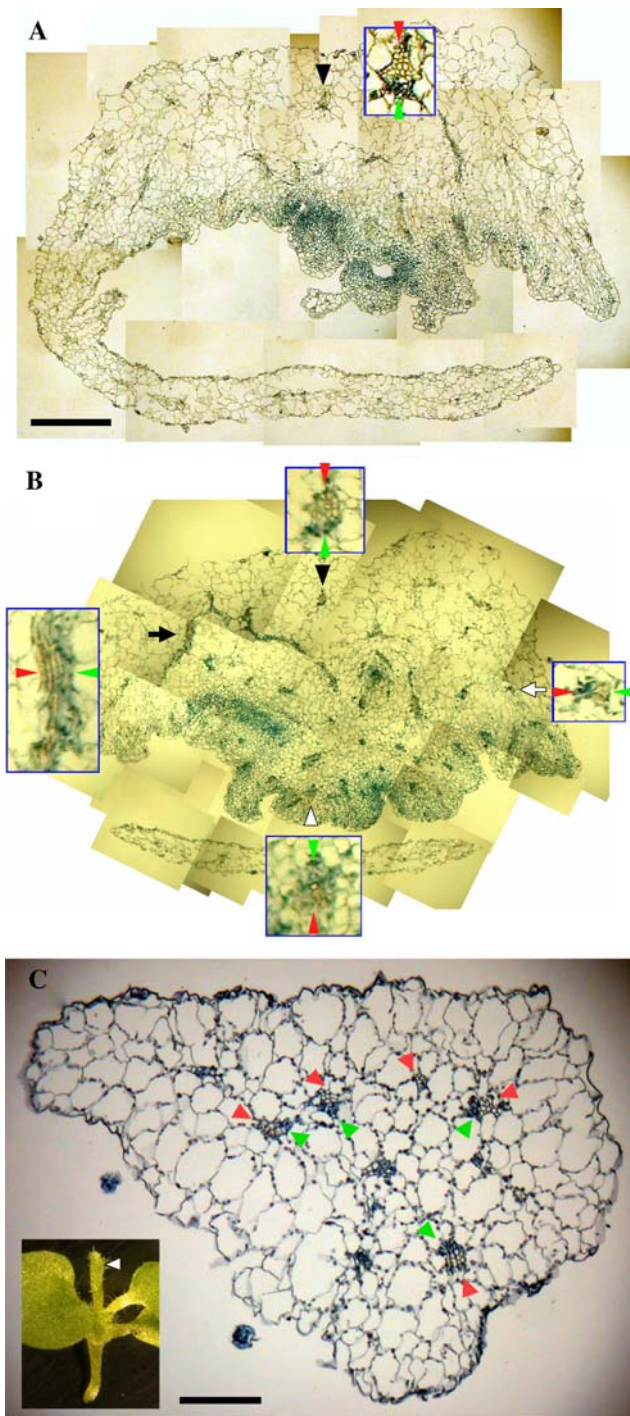
from the numerous small cells in the periphery of the outgrowth of the type 4 cotyledons (Fig. 4B). These results suggested that for the transgenic cotyledons, except for type 1, cell growth occurred preferentially on the abaxial side rather than on the adaxial side (Fig. 4B).

The development of new adventitious vascular bundles proceeded in association with the outgrowths, and close examination of the type 4 outgrowths revealed that the bundles occurred in a dispersed manner without an organized dorsoventral axis. Some veins were formed with their axes perpendicular to the plane of the normal cotyledonous veins (Fig. 4B, arrow in type 4). In the periphery (Fig. 4B) of the blades, some newly formed veins developed a normal longitudinal axis but had an inverted dorsoventral axis in which the phloem formed adaxially and the xylem abaxially. These additional veins were situated face to face with the normal-oriented veins, and thus formed a mirror image (Fig. 4C, colored arrowheads).

Additional transverse sections were made at the middle and top of the type 4 outgrowths (Figs. 5A and B, respectively; diagrams are shown in Fig. 4A). In the latter the outgrowths developed away from the cotyledon blades (see the diagram). Vascular bundles were extensively formed in both middle and top portions but the organization of their veins was distinct from that of the basal portion. At the middle position the vein axes of the outgrowth, situated distal to the cotyledons, were inverted so that the xylem faced the abaxial side and the phloem faced the adaxial side. The axes of the remaining veins were largely random; some were longitudinal and parallel to the plane of the cotyledonous midveins (Fig. 5A), whereas others consisted of veins oriented in several different directions. In contrast, at the position close to the tip, the newly developing veins were predominantly extended parallel to the cotyledonous midveins (Fig. 5B). Veins that developed in the peripheral region of the outgrowth were composed of xylem facing outward and phloem facing inward (Fig. 5B, colored arrowheads). In contrast, the dorsoventral axis of the veins remained unorganized in the central region of the outgrowth. Hence, veins surrounding the central outgrowth had a coordinated, radial distribution pattern.

Distribution of lignin deposition

In association with the modified vascular development there was a prominent deposition of lignin in the transgenic cotyledons in comparison with the wild-type cotyledon blade (Fig. 6A). The deposition was enriched along the bundles and at the periphery of the



◀ **Fig. 5** Histological analysis of type 4 and type 2 outgrowths. **A, B** Transverse sections of the type 4 cotyledon (*6b-S9*) at the intermediate position (**A**, *line m* in Fig. 4A) and at the top position (**B**, *line t* in Fig. 4A). The bulky outgrowth (*upper*) grew larger than the original blade (*lower*). Several representative portions are magnified to clarify the orientation of the vascular bundles. *Solid-black arrowhead*, *open-white arrowhead*, *solid-black arrow*, and *open-white arrow* depict the veins with inverted, normal, right-handed, and left-handed orientations, respectively. *Red* and *green arrowheads* denote xylem and phloem, respectively. The abaxial side corresponds to the upper side of the panel. *Scale bar*: 0.5 mm. Transverse section of a modified epicotyl revealing pin-like protrusions (shown by *white arrowhead* in the inset) that fully developed in the type 2 seedlings after treatment with Dex for 24 days. The *red* and *green arrowheads* denote the xylem and phloem, respectively. *Scale bar*: 0.2 mm



Fig. 6 Lignin in the middle portion of the type 4 outgrowth (panel **A**) and control (panel **B**) cotyledons was stained with phloroglucinol to develop a *brown coloration*. The upper side corresponds to the abaxial side. *Scale bar*: 0.5 mm

outgrowth in the type 4 transgenics and extended toward the periphery of the outgrowths (Fig. 6).

Discussion

Plant tumor formation involves massive cell proliferation and concomitant vascular development to support the growth of the tumorous cells. Here, we have used a

chemically (Dex)-inducible *AK-6b* gene expression system that has enabled us to analyze the process by which tumorous cell growth proceeds and the vascular system develops from normal tissues. The results are exclusively presented for the transgenic line *6b-S9* obtained from *Nicotiana tabacum* cv. Samsun. We previously reported another line *6b-X2* which was obtained from tobacco cultivar Xanthi. Although the growth of Samsun is much different from that of Xanthi (Clement et al. 2006), both *6b-S9* and *6b-X2* lines had a similar set of aberrant and yet distinct morphological types, and therefore morphological, anatomical, and molecular characteristics associated with the line *6b-S9* could be similar to those of the line *6b-X2* (Kakiuchi et al. 2006, data not shown).

Modulation of the dorsoventral axis

Histological analysis of the mature type 4 outgrowths revealed that, at a position close to the petiole, an inverted dorsoventral axis occurred occasionally. It is likely that additional cell layers to generate outgrowths are produced with inverted symmetry. Alternatively, the *AK-6b*-induced outgrowths could have resulted from adaxialization of the abaxial cells. A similar phenotype has been reported for the *phabulosa* and *phavoluta* gain-of-function mutants (McConnell et al. 1998, 2001), which had a reduced level of abaxial cell fate that generated radially symmetrical leaves with the xylem cells surrounding the phloem cells.

The axis formation became more organized at the intermediate position, and then a radial pattern formation emerged at the position close to the tip of outgrowth. This organization was most prominent in the peripheral region, but not evident in the central region of the outgrowths. Supposing that the outgrowth developed acropetally, the spatial differences in patterning could reflect the kinetics of vascular pattern formation. Interestingly, the same xylem/phloem organization was seen in the pin-like protrusions that developed as a result of the modified epicotyl in the type 2 seedlings (Fig. 5c). This orientation is opposite to that observed in vascular bundles of wild-type stems. Helfer et al. (2003) showed that the *AB-6b* gene (derived from strain AB4) induced the formation of green spots on the abaxial side of mature tobacco leaves and that these spots contained normal veins and a second vascular system with inverted orientation on the lower part of the leaf. The *6b* gene in general could, therefore, modulate the dorsoventral axis, and such vascular bundle patterns might be present in the early stages and develop continuously during subsequent stages. The resulting coordinated radial distribution patterns partly resemble those observed in natural crown gall (Aloni et al. 1995), and thus the *6b* gene might affect the development of a specific venation pattern in a natural crown gall.

The knotted-1 type homeobox (*KNOX*) genes play a pivotal role in plant morphogenesis (Lincoln et al. 1994) and *KNOX* gene expression was found to be affected by an auxin transport inhibitor (Scanlon 2003). Considering that reduced polar auxin transport was observed in the *AK-6b*-transgenic seedlings, a putative *KNOX*-like gene in tobacco might be involved in modulating the dorsoventral axis. Indeed, several class I *KNOX* homeobox genes were ectopically expressed in the *AK-6b* transgenic tobacco leaves (Terakura et al. 2006).

In contrast with the radially symmetrical organization of the veins, distribution of small cells of the outgrowths of the type 4 cotyledons was not clearly radially symmetric. The small cells are most probably actively dividing cells, and thus the pattern of vascular formation and cell proliferation might be under the distinct control of development with regard to axis formation.

Possible mechanism of venation pattern formation by the *AK-6b* gene

We have previously shown that the endogenous auxin content of normal and *AK-6b*-transgenic cotyledons was comparable and yet polar auxin transport along hypocotyls was reduced by the action of the *AK-6b* gene (Kakiuchi et al. 2006). It is likely that the *6b* gene induces re-distribution of auxin to generate extensive vein proliferation, because of the modulated auxin transport. It remains to be determined whether cotyledonous auxin transport might also be affected, however, which could be investigated by employing auxin-sensitive reporter genes.

It has been reported that wild-type *Arabidopsis* and tobacco plants treated with auxin-transport inhibitors (Mattsson et al. 1999; Sieburth 1999; An et al. 1999) and *Arabidopsis* auxin transport mutants (Carland and McHale 1996) had branching or fragmented veins and several parallel vascular strands within the petiole and blade. Many of these morphological characteristics were observed in the cotyledon of *AK-6b*-transgenic tobacco.

As noted above, two main hypotheses have been proposed to explain vascular pattern formation: the signal flow canalization hypothesis and the reaction–diffusion (RD) hypothesis, although these are not mutually exclusive. The RD model has been used to explain not only reticulate pattern formation in dicotyledonous leaves but also the striate patterns of monocotyledonous leaves (Nelson and Dengler 1997; Scarpella et al. 2003). Indeed, variations in the values of a single value with an appropriate set of values might result in transition of the pattern from a network pattern to a striate pattern (Asai et al. 1999). From this point of view, the unique venation pattern formation of the *AK-6b*-tobacco could be explained by an RD model at least at the early stages of modulated vein pattern formation. The *AK-6b*-tobacco seedlings had a modulated reticulate (network) pattern in the type 2 cotyledons, and a striated (striped) pattern in both the type 3 and 4 cotyledons. Interestingly, the intermediate patterns produced by the model proposed by Asai et al. (1999) includes wavy stripes and a more complex spotted

(network) pattern, both of which were observed in transgenic AK-6b-tobacco, suggesting that RD dynamics is a plausible mechanism for developing the cotyledon venation patterns. Grémillon et al. (2004) also showed the occurrence of crinkly secondary veins in young tobacco leaves expressing T-6b gene from the Tm4 strain.

To construct a genuine RD model for cotyledon vein pattern formation, it is necessary to find substances acting as “activator(s)” and “inhibitor(s)” of vein pattern formation. It is likely that auxin will be a primary candidate of such an activator, because redistribution of auxin could be involved in massive vascular development as we suggested above. Grémillon et al. (2004) reported that the 6b gene (T-6b) product was diffusible between tissues, causing enation syndromes in transgenic tobacco. On the basis of this observation, 6b protein itself might be involved in the reaction–diffusion dynamics. Although this report seems to support RD model, our results do not rule out the flow canalization hypothesis.

In natural crown gall tumors, both auxin and cytokinin accumulate abundantly as a result of expression of biosynthesis genes in the T-DNA, and hence these plant-growth substances, apart from the 6b gene product, are undoubtedly important and could be a prerequisite for initiation of vein development. Accordingly, in natural crown galls the 6b gene may not act in generation of veins but may modulate pattern formation of the veins.

Precise determination of the intrinsic activity of the AK-6b protein has been hampered, partly because of the lack of a prominent motif in the amino acid sequence. Kitakura et al. (2002) proposed that the 6b protein is a transcriptional regulator which modulates the gene expression profile to cause morphological alterations in plants. Clément et al. (2006) reported a new finding that T-6b acts as an osmoregulator by increasing synthesis of sugars, causing cell expansion. Gális et al. (2004) proposed that the AK-6b protein could be associated with reactions generating CoA derivatives which lead to massive phenylpropanoid synthesis. Flavonoids among the resulting phenolic compounds could be the auxin-transport inhibitors (Kakiuchi et al. 2006) which are probably responsible for AK-6b-induced phenotypic alterations. On the basis of these observations it is possible that 6b protein itself, or by interaction with putative transcription factors, modulates transcriptional patterns of both phenylpropanoids and sugar biosynthesis gene expression.

Acknowledgments We thank Drs S. Youssefian (Akita Prefectural University) and I. Gális (RIKEN) for critical reading of

the manuscript, and Dr A. Ogawa for technical guidance with histochemical analysis. This work was partly supported by the Sasagawa Scientific Research Grant from the Japan Science Society (No. 13–238).

References

- Akiyoshi DE, Klee H, Amasino RM, Nester EW, Gordon MP (1984) T-DNA of *Agrobacterium tumefaciens* encodes an enzyme of cytokinin biosynthesis. Proc Natl Acad Sci USA 81:5994–5998
- Aloni R (1995) The induction of vascular tissues by auxin and cytokinin. In: Davies P (eds) Plant hormones. physiology, biochemistry and molecular biology. Kluwer Academic, Dordrecht, pp 531–546
- Aloni R, Pradel KS, Ullrich CI (1995) The three-dimensional structure of vascular tissues in *Agrobacterium tumefaciens*-induced crown galls and in the host stems of *Ricinus communis* L. Planta 196:597–605
- An ND, Wang LJ, Xu ZH, Xia ZA (1999) Foliar modifications induced by inhibition of polar transport of auxin. Cell Res 9:27–35
- Aoyama T, Chua NH (1997) A glucocorticoid-mediated transcriptional induction system in transgenic plants. Plant J 11:605–612
- Asai R, Taguchi E, Kume Y, Saito M, Kondo S (1999) Zebrafish *Leopard* gene as a component of the putative reaction-diffusion system. Mech Dev 89:87–92
- Carland FM, McHale NA (1996) *LOPI*: a gene involved in auxin transport and vascular patterning in *Arabidopsis*. Development 122:1811–1819
- Chilton M-D, Drummond MH, Merlo DJ, Sciaky D, Montoya AL, Gordon MP, Nester EW (1977) Stable incorporation of plasmid DNA into higher plant cells: the molecular basis of crown gall tumorigenesis. Cell 11:263–271
- Clément B, Pollmann S, Weiler E, Urbanczyk-Wochniak E, Otten L (2006) The *Agrobacterium vitis* T-6b oncoprotein induces auxin-independent cell expansion in tobacco. Plant J 45:1017–1027
- Feugier FG, Mochizuki A, Iwasa Y (2005) Self-organization of the vascular system in plant leaves: inter-dependent dynamics of auxin flux and carrier proteins. J Theor Biol 236:366–375
- Fukuda H (1992) Tracheary element formation as a model system of cell differentiation. Int Rev Cytol 136:289–332
- Gális I, Šimek P, Macas J, Zahradníčková H, Vlasák J, Wabiko H, Van Dongen W, Van Onckelen HA, Ondřej M (1999) The *Agrobacterium tumefaciens* C58-6b gene confers resistance to N⁶-benzyladenine without modifying cytokinin metabolism in tobacco seedlings. Planta 209:453–461
- Gális I, Šimek P, Van Onckelen HA, Kakiuchi Y, Wabiko H (2002) Resistance of transgenic tobacco seedlings expressing the *Agrobacterium tumefaciens* C58-6b gene, to growth-inhibitory levels of cytokinin is associated with elevated IAA levels and activation of phenylpropanoid metabolism. Plant Cell Physiol 43:939–950
- Gális I, Kakiuchi Y, Šimek P, Wabiko H (2004) *Agrobacterium tumefaciens* AK-6b gene modulates phenolic compound metabolism in tobacco. Phytochemistry 65:169–179
- Grémillon L, Helfer A, Clément B, Otten L (2004) New plant growth-modifying properties of the *Agrobacterium* T-6b oncogene revealed by the use of a dexamethasone-inducible promoter. Plant J 37:218–228
- Helfer A, Clément B, Michler P, Otten L (2003) The *Agrobacterium* oncogene AB-6b causes a graft-transmissible enation syndrome in tobacco. Plant Mol Biol 52:483–493

- Hooykaas PJJ, den Dulk-Ras H, Schilperoort RA (1988) The *Agrobacterium tumefaciens* T-DNA gene 6^b is an *onco* gene. *Plant Mol Biol* 11:791–794
- Jacobs M, Rubery PH (1988) Naturally occurring auxin transport regulators. *Science* 241:346–349
- Kakiuchi Y, Gális I, Tamogami S, Wabiko H (2006) Reduction of polar auxin transport in tobacco by the tumorigenic *Agrobacterium tumefaciens* AK-6b gene. *Planta* 223:237–247
- Kitakura S, Fujita T, Ueno Y, Terakura S, Wabiko H, Machida Y (2002) The protein encoded by oncogene 6b from *Agrobacterium tumefaciens* interacts with a nuclear protein of tobacco. *Plant Cell* 14:451–463
- Körber H, Strizhov N, Staiger D, Feldwisch J, Olsson O, Sandberg G, Palme K, Schell J, Koncz C (1991) T-DNA gene 5 of *Agrobacterium* modulates auxin response by autoregulated synthesis of a growth hormone antagonist in plants. *EMBO J* 10:3983–3991
- Koizumi K, Sugiyama M, Fukuda H (2000) A series of novel mutants of *Arabidopsis thaliana* that are defective in the formation of continuous vascular network: calling the auxin signal flow canalization hypothesis into question. *Development* 127:3197–3204
- Lincoln C, Long J, Yamaguchi J, Serikawa K, Hake S (1994) A *knotted1*-like homeobox gene in *Arabidopsis* is expressed in the vegetative meristem and dramatically alters leaf morphology when overexpressed in transgenic plants. *Plant Cell* 6:1859–1876
- Mattsson J, Sung ZR, Berleth T (1999) Responses of plant vascular systems to auxin transport inhibition. *Development* 126:2979–2991
- Mattsson J, Ckurshumova W, Berleth T (2003) Auxin signaling in *Arabidopsis* leaf vascular development. *Plant Physiol* 131:1327–1339
- McConnell JR, Barton MK (1998) Leaf polarity and meristem formation in *Arabidopsis*. *Development* 125:2935–2942
- McConnell JR, Emery J, Eshed Y, Bao N, Bowman J, Barton MK (2001) Role of *PHABULOSA* and *PHAVOLUTA* in determining radial patterning in shoots. *Nature* 411:709–713
- Meinhardt H (1982) *Models of biological pattern formation*. Academic, London
- Nelson T, Dengler N (1997) Leaf vascular pattern formation. *Plant Cell* 9:1121–1135
- Sachs T (1981) The control of patterned differentiation of vascular tissues. *Adv Bot Res* 9:151–262
- Sachs T (1989) The development of vascular networks during leaf development. *Current Topics Plant Biochem Physiol* 8:168–183
- Scanlon MJ (2003) The polar auxin transport inhibitor N-1-naphthylphthalamic acid disrupts leaf initiation, KNOX protein regulation, and formation of leaf margins in maize. *Plant Physiol* 133:597–605
- Scarpella E, Rueb S, Meijer AH (2003) The *RADICLELESS1* gene is required for vascular pattern formation in rice. *Development* 130:645–658
- Schröder G, Waffenschmidt S, Weiler EW, Schröder J (1984) The T-region of Ti plasmids codes for an enzyme synthesizing indole-3-acetic acid. *Eur J Biochem* 138:387–391
- Sieburth LE (1999) Auxin is required for leaf vein pattern in *Arabidopsis*. *Plant Physiol* 121:1179–1190
- Spanier K, Schell J, Schreier PH (1989) A functional analysis of T-DNA gene 6b: The fine tuning of cytokinin effects on shoot development. *Mol Gen Genet* 219:209–216
- Terakura S, Kitakura S, Ishikawa M, Ueno Y, Fujita T, Machida C, Wabiko H, Machida Y (2006) Oncogene 6b from *Agrobacterium tumefaciens* induces abaxial cell division at late stages of leaf development and modifies vascular development in petioles. *Plant Cell Physiol* 47:664–672
- Thomashow LS, Reeves S, Thomashow MF (1984) Crown gall oncogenesis: evidence that a T-DNA gene from the *Agrobacterium* Ti plasmid pTiA6 encodes an enzyme that catalyzes synthesis of indoleacetic acid. *Proc Natl Acad Sci USA* 81:5071–5075
- Thomashow MF, Hugly S, Buchholz WG, Thomashow LS (1986) Molecular basis for the auxin-independent phenotype of crown gall tumor tissues. *Science* 231:616–618
- Tinland B, Huss B, Paulus F, Bonnard G, Otten L (1989) *Agrobacterium tumefaciens* 6b genes are strain-specific and affect the activity of auxin as well as cytokinin genes. *Mol Gen Genet* 219:217–224
- Van Larebeke N, Engler G, Holsters M, Van Den Elsacker S, Zaenen I, Schilperoort RA, Schell J (1974) Large plasmid in *Agrobacterium tumefaciens* essential for crown gall-inducing ability. *Nature* 252:169–170
- Van Onckelen HA, Prinsen E, Inzé D, Rüdelsheim PL, Van Lijsebettens M, Follin A, Schell J, Van Montagu M, DeGreef JA (1986) *Agrobacterium* T-DNA gene 1 codes for tryptophan-2-monooxygenase activity in tobacco crown gall cells. *FEBS Lett* 198:357–360
- Wabiko H, Minemura M (1996) Exogenous phytohormone-independent growth and regeneration of tobacco plants transgenic for the 6b gene of *Agrobacterium tumefaciens* AKE10. *Plant Physiol* 112:939–951